Recent results based on continuous GPS observations of the GIA process in Fennoscandia from BIFROST

Martin Lidberg, Jan M. Johansson, Hans-Georg Scherneck, Glenn A. Milne

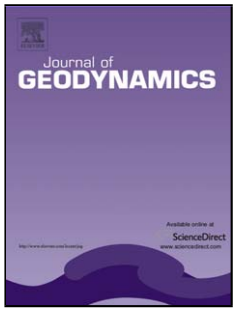

Title: Recent results based on continuous GPS observations of the GIA process in Fennoscandia from BIFROST

Authors: Martin Lidberg, Jan M. Johansson, Hans-Georg Scherneck, Glenn A. Milne

PII: S0264-3707(09)00166-5
DOI: doi:10.1016/j.jog.2009.11.010
Reference: GEOD 959

To appear in: *Journal of Geodynamics*

Received date: 17-2-2009
Revised date: 20-11-2009
Accepted date: 21-11-2009

Please cite this article as: Lidberg, M., Johansson, J.M., Scherneck, H.-G., Milne, G.A., Recent results based on continuous GPS observations of the GIA process in Fennoscandia from BIFROST, *Journal of Geodynamics* (2008), doi:10.1016/j.jog.2009.11.010

Revised and resubmitted to Journal of Geodynamics 2009-11-05

Least-squares modification of extended Stokes' formula and its second-order radial derivative for validation of satellite gravity gradiometry data

Mehdi Eshagh
Division of Geodesy, Royal Institute of Technology, Stockholm, Sweden
Tel:+4687907369; Fax:+4687907343
Email:eshagh@kth.se

Abstract The gravity anomalies at sea level can be used to validate the satellite gravity gradiometry data. Validation of such a data is important prior to downward continuation because of amplification of the data errors through this process. In this paper the second-order radial derivative of the extended Stokes' formula is employed and the emphasis is on least-squares modification of this formula to generate the second-order radial gradient at satellite level. Two methods in this respect are proposed: a) modifying the second-order radial derivative of extended Stokes' formula directly, b) modifying extended Stokes' formula prior to taking the second-order radial derivative. Numerical studies show that the former method works well but the latter is very sensitive to the proper choice of the cap size of integration and degree of modification.

Keywords: Biased, unbiased, optimum estimator, global root mean square error, truncation error, error spectra, signal spectra

1 Introduction

The satellite gravity gradiometry (SGG) is a technique to measure second-order derivatives of the Earth's gravity field from space. It is expected to determine the geopotential coefficients to higher degrees and orders than those are obtained from other satellite techniques. The SGG data can be used to study the geophysical/geodynamical phenomena as well. Quality of the data is important, as occurrence of any error in the data will lead to a wrong interpretation and unrealistic conclusions for the phenomena. Therefore, the quality of SGG data should be controlled prior to use, or in other words, the data should be validated.

Different methods of validating SGG data have been proposed. A simple way could be the direct comparison of the real SGG data with the synthesized gravitational gradients using an existing Earth's gravitational model (EGM). Another idea is to use regional gravity data to generate the gradients at satellite level. Haagmans et al. (2002) and Kern and Haagmans (2004) used the extended Stokes formula (ESF) and extended Hotine formula to generate the gravitational gradients using terrestrial gravity data. Denker (2002) used the least-squares spectral combination technique to generate and validate the gravitational gradients. Bouman et al. (2003) has set up a calibration model based on instrument (gradiometer) characteristics to validate the measurements. Mueller et al. (2004) used the terrestrial gravity anomalies to generate the gravitational gradients, and after that Wolf (2007) investigated the deterministic approaches to modify the integrals and validate the SGG data. In fact, the spectral weighting scheme (Sjöberg 1980 and 1981 and Wenzel 1981) was used by Wolf

(2007). Stochastic methods of modifying Stokes' formula, or in other words least-squares modification (LSM) can be used for the extended Stokes formula as well; see Sjöberg (1984a), (1984b), (1991) and (2003). Least-squares collocation can be used for validation purposes. Tscherning et al. (2006) considered this method and concluded that the gradients can be predicted with an error of 2-3 mE in the case of an optimal size of the collection area and optimal resolution of data. Zielinski and Petrovskaya (2003) proposed a balloon-borne gradiometer to fly at 20-40 km altitude simultaneously with satellite mission and proposed downward continuation of satellite data and comparing them with balloon-borne data. Bouman and Koop (2003) presented an along-track interpolation method to detect the outliers. Their idea is to compare the along-tack interpolated gradients with measured gradients. If the interpolation error is small enough the differences should be predicted reasonably by an error model. Pail (2003) proposed a combined adjustment method supporting high quality gravity field information within the well-surveyed test area for continuation of local gravity field upward and validating the SGG data. Bouman et al. (2004) stated that there are some limitations in generating the gravitational gradients using terrestrial gravimetry data and EGMs. When an EGM model is used, high degrees and orders should be taken into account and the recent EGMs seem to be able to remove the greater part of the systematic errors. In their regional approach they concluded that the bias of the gradients can accurately be recovered using least-squares collocation. Also, they concluded that the method of validation using high-low satellite-to-satellite tracking data fails unless a higher resolution EGM is available. Kern and Haagmans (2004) and Kern et al. (2005) presented an algorithm for detecting the outliers in the SGG data in the time domain.

The second-order radial derivative (SORD) of extended Stokes' kernel (ESK) is isotropic and azimuth-independent. The isotropy is an important property in modifying ESF otherwise it will not be an easy task. Two methods of generating the SGG data are investigated in this paper, in the first method (Method 1), the SORD of ESF is modified (derivative prior to modification) and in the second method (Method 2) ESF is modified and after that the SORD is taken (modification prior to derivative). Modification of ESF and its SORD based on the biased LSM (BLSM), unbiased LSM (ULSM) and optimum LSM (OLSM) are the main subject of this study which is a new issue in the scope of SGG. Obviously, Methods 1 and 2 will not deliver the same results, but we are going to test in which cases these methods are comparable. We select the SORD of ESF as its kernel function is isotropic, in such a case, we can use both methods to generate the second-order radial gradient and compare the results. The importance of this study is mostly related to Method 2 although Method 1 (based on the LSM) is new as well. If we can find the cases, where Method 2 performs well, the method can be used to some how modify the horizontal derivatives of ESF having non-isotropic kernels, to generate the other gradients. A similar study was done by Wolf (2007) but just based on deterministic approaches. However we concentrate on generating the second-order radial gradient based on the LSM approaches.

The disturbing potential can be expressed by an integral which is well-known as ESF. This integral formula is (Heiskanen and Moritz 1967):

$$T(P)=\frac{R}{4\pi}\iint_{\sigma} S(r,\psi)\Delta g(Q)d\sigma\,, \tag{1a}$$

where R is the radius of the reference sphere, r is the geocentric distance at computation point P, ψ is the geocentric angle between the computation point P and the integration point Q with the following expression:

$$\cos\psi=\cos\theta\cos\theta'+\sin\theta\sin\theta'\cos(\lambda'-\lambda), \tag{1b}$$

and θ and λ are the co-latitude and longitude of P and θ' and λ' are of the integration point Q. σ is the unit sphere, $\Delta g(Q)$ is the gravity anomaly at sea level and

$$S(r,\psi)=\sum_{n=2}^{\infty}\frac{2n+1}{2}\Omega_n(r)P_n(\cos\psi), \tag{1c}$$

is the spectral form of ESK with the spectrum:

$$\Omega_n(r)=\frac{2}{n-1}\left(\frac{R}{r}\right)^{n+1}. \tag{1d}$$

Equation (1a) shows that the integration should be performed globally, which means that $\Delta g(Q)$ with a global coverage is required. Therefore we should look for an approach to modify the integral in such a way that the contribution of the far zone data is minimized. Different methods for modifying Stokes' formula have been presented, but here the concentration is on the stochastic approaches of Sjöberg (1984a) and (1984b). In fact, the theory behind this part of the study was presented by him, but just on Stokes' integral for geoid determination. However, we are going to test the capability of these stochastic approaches in modifying ESF and its SORD and generating the SGG data for validation purposes. In the following we investigate the LSM of ESF.

2 LSM of ESF

The general estimator of the disturbing potential based on ESF is very similar to the general geoid estimator of Sjöberg (2003); and the only difference is related to the kernel function and its spectrum. Let us start the discussion by this general disturbing potential estimator:

$$\tilde{T}(P)=\frac{R}{4\pi}\iint_{\sigma_0} S^{L}(r,\psi)\Delta g^{\mathrm{T}}(Q)d\sigma+\frac{R}{2}\sum_{n=2}^{L}b_n(r)\Delta g_n^{\mathrm{EGM}}(P), \tag{2a}$$

where L is the maximum degree of modification, $b_n(r)$ is a parameter which differs with the type of the LSM, and

$$S^L(r,\psi) = S(r,\psi) - \sum_{n=2}^{L} \frac{2n+1}{2} s_n(r) P_n(\cos\psi), \tag{2b}$$

is the modified ESF and $s_n(r)$ are the modification parameters, which are estimated. The closed form formula of this function is (Heiskanen and Moritz 1967, p. 93, Eq. 2-162):

$$S(r,\psi) = \frac{2R}{l} + \frac{R}{r} - 3\frac{Rl}{r^2} - \frac{R^2}{r^2}\cos\psi\left(5 + 3\ln\frac{r - R\cos\psi + l}{2r}\right), \tag{2c}$$

where

$$l = \sqrt{r^2 + R^2 - 2Rr\cos\psi}\,, \tag{2d}$$

is the spatial distance between the points P and Q. $\Delta g_n^{\mathrm{EGM}}(P)$ is the Laplace harmonic expansion of $\Delta g(P)$ (Heiskanen and Moritz 1967, p. 97). In order to show from which sources the gravity anomaly is derived we separate them into Δg^{T} for the terrestrial and Δg^{EGM} for the EGM based data.

The LSM parameters $s_r(r)$ are derived based on solving the following system of equations (Sjöberg 2003):

$$\sum_{r=2}^{M} a_{kr} s_r(r) = h_k(r), \quad k = 2, 3, \ldots, M, \tag{2e}$$

where mathematical forms of a_{kr} and $h_k(r)$ depend on type of the LSM which is used.

Equation (2e) differs with the system of equations in which the modification parameters of the Stokes formula is used for geoid determination. As Eq. (2e) shows both sets of the modification parameters and the truncation coefficients are altitude-dependent and variable with the elevation of the computation point P. We will investigate the changes in these parameters and coefficients in Section 4. The mathematical formula of the elements of coefficient matrix and the right hand side vector of Eq. (2e) depend on the method of the LSM. In the following we summarized them in three propositions.

Proposition 1 *The BLSM parameters for the disturbing potential estimator at satellite level are derived by setting* $b_n(r) = s_n(r)$ *and solving the system of equations Eq. (2e) with the following elements (Sjöberg 2003)*:

$$a_{kr} = a_{rk} = \left(\sigma_r^2 + dc_r\right)\delta_{kr} - E_{kr}\left(\psi_0\right)\sigma_r^2 - E_{rk}\left(\psi_0\right)\sigma_k^2 + \\ + \sum_{n=2}^{\infty} E_{nr}\left(\psi_0\right)E_{nk}\left(\psi_0\right)\left(\sigma_n^2 + c_n\right)$$

$$h_k\left(r\right) = \left[\Omega_k\left(r\right) - Q_k\left(r,\psi_0\right)\right]\sigma_k^2 + \\ + \sum_{n=2}^{\infty}\left[Q_n\left(r,\psi_0\right)\left(\sigma_n^2 + c_n\right) - \Omega_k\left(r\right)\sigma_n^2\right]E_{nk}\left(\psi_0\right).\ k\,,\ r = 2,\,3,\ldots,\,M$$

where

$$E_{rk}\left(\psi_0\right) = \frac{2k+1}{2}e_{rk}\left(\psi_0\right)\,, \tag{3a}$$

$$e_{rk}\left(\psi_0\right) = \int_{\psi_0}^{\pi} P_r\left(\cos\psi\right)P_k\left(\cos\psi\right)\sin\psi d\psi\,, \tag{3b}$$

$$Q_k\left(r,\psi_0\right) = \int_{\psi_0}^{\pi} S\left(r,\psi\right)P_k\left(\cos\psi\right)\sin\psi d\psi\,, \tag{3c}$$

$$Q_k\left(r,\psi_0\right) = \sum_{n=2}^{\infty}\frac{2n+1}{2}\Omega_n\left(r\right)e_{nn'}\left(\psi_0\right). \tag{3d}$$

where σ_k^2 is the error spectrum of the terrestrial gravimetric data and dc_k is the error spectrum of the gravity anomaly obtained from an existing EGM.

For more details about the computation of σ_k^2 the reader is referred e.g. to Sjöberg (1991), Ågren (2004) and Ellmann (2005). The spectrum of the gravity anomaly is evaluated by using an EGM for those degrees below the maximum degree of modification, and analytical models like Kaula (1963), Tscherning and Rapp (1974) are used for the degrees above that maximum degree. According to Ellmann (2004) and (2005) and Ågren (2004) the Tscherning-Rapp model is superior with respect to the others. Relying on their conclusion we use this model in our numerical studies through this paper. $Q_k\left(r,\psi_0\right)$ and $e_{nn'}\left(\psi_0\right)$ are the truncation error coefficients of ESK and the Paul coefficients (Paul 1978), respectively.

Proposition 2 *The ULSM parameters of the disturbing potential estimator at satellite level are derived, if we select $b_n\left(r\right) = Q_n^L\left(r,\psi_0\right) + s_n\left(r\right)$ and solve the system of Eq. (2e) with the following elements (Sjöberg 2003)*:

$$a_{kr} = a_{rk} = d_r\delta_{kr} - E_{rk}\left(\psi_0\right)d_r - E_{kr}\left(\psi_0\right)d_k + \sum_{n=2}^{\infty}E_{nr}\left(\psi_0\right)E_{nk}\left(\psi_0\right)d_n\,,$$

$$h_k\left(r\right) = \Omega_k\left(r\right)\sigma_k^2 - Q_k\left(r,\psi_0\right)d_k + \sum_{n=2}^{\infty}\left[Q_n\left(r,\psi_0\right)d_n - \Omega_n\left(r\right)\sigma_n^2\right]E_{nk}\left(\psi_0\right),$$

$$k\,,\ r = 2,\,3,\ldots,\,M$$

where

$$d_n = \sigma_n^2 + dc_n .$$

Proposition 3 *The OLSM parameters of the disturbing potential estimator at satellite level are derived, if we set* $b_n(r) = \left[Q_n^L(r,\psi_0) + s_n(r)\right] c_n / (c_n + dc_n)$ *and solve Eq. (2e) with the following elements (Sjöberg 2003)*:

$$a_{kr} = a_{rk} = C_r \delta_{kr} - E_{rk}(\psi_0) C_r - E_{kr}(\psi_0) C_k + \sum_{n=2}^{\infty} E_{nr}(\psi_0) E_{nk}(\psi_0) C_n ,$$
$$k, r = 2, 3, \ldots, M$$

$$h_k(r) = \Omega_k(r)\sigma_k^2 - Q_k(r,\psi_0) C_k + \sum_{n=2}^{\infty} \left[Q_n(r,\psi_0) C_n - \Omega_n(r)\sigma_n^2\right] E_{nk}(\psi_0) .$$

where

$$C_k = \sigma_k^2 + \begin{cases} c_k dc_k / (c_k + dc_k) & 2 \le k \le M \\ c_k & k > M \end{cases} , \tag{4a}$$

$$Q_n^L(r,\psi_0) = Q_n(r,\psi_0) - \sum_{k=2}^{L} s_n(r) E_{nk}(\psi_0) . \tag{4b}$$

3 LSM of the SORD of ESF

The gravitational tensor is a symmetric tensor with 5 independent elements. This tensor is also traceless (trace of this tensor is zero) since the disturbing potential is harmonic outside the Earth's surface. Therefore, if we present a method for validating the simplest components, such as $T_{zz}(P) = T_{rr}(P)$, in fact we validate $T_{xx}(P) + T_{yy}(P)$, too. If $T_{rr}(P)$ is not equal to $-T_{xx}(P) - T_{yy}(P)$, it means that there is error either in $T_{rr}(P)$ or $-T_{xx}(P) - T_{yy}(P)$. Assuming the former is free of error, we conclude that the latter is erroneous, but we cannot say which one of the components $-T_{xx}(P)$ and $-T_{yy}(P)$ contains the blunder. In this section similar to the previous one we consider the LSM method of modifying the SORD of ESF to generate $T_{rr}(P)$ at point P at satellite level. We define the following general estimator $\tilde{T}_{rr}(P)$:

$$\tilde{T}_{rr}(P) = \frac{R}{4\pi} \iint_{\sigma_0} S_{rr}^L(r,\psi) \Delta g^{\mathrm{T}}(Q) d\sigma + \frac{R}{2} \sum_{n=2}^{L} b_n''(r) \Delta g_n^{\mathrm{EGM}}(P) , \tag{5a}$$

where $b_n''(r)$ is a parameter that should be estimated according to the type of estimator, and

$$S_{rr}^{L}(r,\psi)=S_{rr}(r,\psi)-\sum_{n=2}^{L}\frac{2n+1}{2}s_n''(r)P_n(\cos\psi), \tag{5b}$$

where $s_n''(r)$ are the modification parameters to be estimated, and (Reed 1973, Eq. 5.35)

$$S_{rr}(r,\psi)=\frac{t^3}{R^2}\left\{(1-t\cos\psi)\left[\frac{3(1-t^2)}{D^5}-\frac{4}{D^3}\right]-\frac{1+t^2}{D^3}-\frac{10}{D}-18D+\right.$$
$$\left.+2-3t\cos\psi\left(15+6\ln\frac{1-t\cos\psi+D}{2}\right)\right\}, \tag{5c}$$

where $t=R/r$ and $D=\sqrt{1-2t\cos\psi+t^2}$.

The LSM of SORD of ESF is very similar to that of ESF itself. If we estimate the modification parameter $s_n''(r)$, the left hand side of the system of equations (Eq. 2e) will not change and remain the same with those presented for the LSM of ESF. In such a case only the right hand side of Eq. (2e) will change. In the following, we present how the modification parameters $s_n''(r)$ are estimated. At the first step, we start with the following corollary which is related with the BLSM of the SORD of ESF.

Corollary 1 *The BLSM parameters are derived by setting $b_n''(r)=s_n''(r)$ and solving the system of equations Eq. (2e) with the following right hand side*

$$h_k(r)=\left\{\Omega_k''(r)-\left[Q_k(r,\psi_0)\right]_{zz}\right\}\sigma_k^2+$$
$$+\sum_{n=2}^{\infty}\left[\left[Q_k(r,\psi_0)\right]_{zz}\left(\sigma_n^2+c_n\right)-\Omega_k''(r)\sigma_n^2\right]E_{nk}(\psi_0), \tag{6a}$$

where

$$\left[Q_k(r,\psi_0)\right]_{rr}=\int_{\psi_0}^{\pi}S_{rr}(r,\psi)P_k(\cos\psi)\sin\psi d\psi, \tag{6b}$$

or in spectral form

$$\left[Q_k(r,\psi_0)\right]_{rr}=\sum_{n=2}^{\infty}\frac{2n+1}{2}\Omega_n''(r)e_{nk}(\psi_0), \tag{6c}$$

where

$$\Omega_n''(r)=\frac{(n+1)(n+2)}{r^2}\Omega_n(r), \tag{6d}$$

where $\Omega_n(r)$ was introduced in Eq. (1d).

Proof. The only difference between the biased geoid estimator of Sjöberg (1991) and the biased T_{rr} estimator is related to the truncation coefficients and spectrum of the SORD of ESF. If we consider the errors of terrestrial and satellite data by ε^{T} and $\varepsilon_n^{\mathrm{EGM}}$, respectively, we can write the following estimator for the error of T_{rr}:

$$\delta\tilde{T}_{rr}(P)=\frac{R}{4\pi}\iint_{\sigma_0}S_{rr}^{L}(r,\psi)\varepsilon^{\mathrm{T}}(Q)d\sigma+\frac{R}{2}\sum_{n=2}^{L}s_n''(r)\varepsilon_n^{\mathrm{EGM}}(P). \tag{7}$$

Sjöberg (1991) proved that the integral part of this equation has the following spectral form

$$\frac{R}{4\pi}\iint_{\sigma_0}S_{rr}^{L}(r,\psi)\varepsilon^{T}(Q)d\sigma=\frac{R}{2}\sum_{n=2}^{\infty}\left\{\Omega_n''(r)-s_n''^{*}(r)-\left[Q_n^{L}(r,\psi_0)\right]_{rr}\right\}\varepsilon_n^{\mathrm{T}}, \tag{8a}$$

where

$$\left[Q_n^{L}(r,\psi_0)\right]_{rr}=\left[Q_n(r,\psi_0)\right]_{rr}-\sum_{k=2}^{L}s_k''(r)E_{nk}(\psi_0). \tag{8b}$$

Substituting Eq. (8a) into Eq. (7) we obtain

$$\delta\tilde{T}_{rr}(P)=\frac{R}{2}\sum_{n=2}^{\infty}\left\{\Omega_n''(r)-s_n''^{*}(r)-\left[Q_n^{L}(r,\psi_0)\right]_{rr}\right\}\varepsilon_n^{\mathrm{T}}(P)+\frac{R}{2}\sum_{n=2}^{L}s_n''(r)\varepsilon_n^{\mathrm{EGM}}(P). \tag{8c}$$

By considering that the errors are random with zero stochastic expectation:

$$E\left(\varepsilon_n^{\mathrm{T}}\right)=E\left(\varepsilon_n^{\mathrm{EGM}}\right)=0, \tag{8d}$$

we have

$$E\left\{\delta\tilde{T}_{rr}^{2}\right\}=E\left\{\frac{1}{4\pi}\iint_{\sigma}\delta T_{rr}^{2}d\sigma\right\}=$$

$$=\frac{R^2}{4}\sum_{n=2}^{L}\left\{\left\{\Omega_n''(r)-s_n''(r)-\left[Q_n^{L}(r,\psi_0)\right]_{rr}\right\}^2\sigma_n^2+\left[Q_n^{L}(r,\psi_0)\right]_{rr}^2c_n+s_n''^{2}(r)dc_n\right\}+$$

$$+\frac{R^2}{4}\sum_{n=M+1}^{\infty}\left\{\left\{\Omega_n''(r)-\left[Q_n^{L}(r,\psi_0)\right]_{rr}\right\}^2\sigma_n^2+\left[Q_n^{L}(r,\psi_0)\right]_{rr}^2c_n\right\}. \tag{8e}$$

By differentiating Eq. (8e) with respect to $s_k''(r)$ and equating the result to zero and rearranging the known and the unknown parameters $s_k''(r)$, the corollary is proved.

Corollary 2 *The ULSM parameters* $s_n''(r)$ *are derived by considering* $b_n''(r)=\left\{\left[Q_n^L(r,\psi_0)\right]_{rr}+s_n''(r)\right\}$ *and solving the system of equations Eq. (2e) by considering*

$$h_k(r)=\Omega_k''(r)\sigma_k^2-\left[Q_k(r,\psi_0)\right]_{rr}d_k+\sum_{n=2}^{\infty}\left\{\left[Q_k(r,\psi_0)\right]_{rr}d_n-\Omega_n''(r)\sigma_n^2\right\}E_{nk}(\psi_0).$$

Proof. Similar to the proof presented for Corollary 1 we can write the error estimator as:

$$\begin{aligned}\delta\tilde{T}_{rr}(P)=&\frac{R}{4\pi}\iint_{\sigma_0}S_{rr}^L(r,\psi)\varepsilon^{\mathrm{T}}(Q)d\sigma+\frac{R}{2}\sum_{n=2}^{M}\left\{\left[Q_n^L(r,\psi_0)\right]_{rr}+s_n''(r)\right\}\varepsilon_n^{\mathrm{EGM}}(P)-\\&-\frac{R}{2}\sum_{n=M+1}^{L}\left\{\left[Q_n^L(r,\psi_0)\right]_{rr}+s_n''(r)\right\}\Delta g_n^T(P)-\frac{R}{2}\sum_{n=L+1}^{\infty}\left[Q_n^L(r,\psi_0)\right]_{rr}\Delta g_n^T(P),\end{aligned}\tag{9a}$$

where $\left[Q_n^L(r,\psi_0)\right]_{rr}$ was already presented in Eq. (8b). The mathematical expectation of Eq. (9a) shows that the estimator is unbiased through *M*, which is in fact the maximum degree of the EGM for generating the long wavelength structure of the estimator. By squaring the above equation and considering that the EGM and terrestrial data are not correlated and after taking the statistical expectation and the global average, as we did in Eq. (8e), we have the following spectral form for the global mean squares error:

$$\begin{aligned}E\left\{\delta\tilde{T}_{rr}^2\right\}=\frac{R^2}{4}\sum_{n=2}^{\infty}\Bigg\{&\left\{\Omega_n''(r)-s_n''^{*}(r)-\left[Q_n^L(r,\psi_0)\right]_{rr}\right\}^2\sigma_n^2+\\&+\left\{\left[Q_n^L(r,\psi_0)\right]_{rr}+s_n''^{*}(r)\right\}^2\Bigg\}dc_n^*,\end{aligned}\tag{9b}$$

where

$$s_n''^{*}(r)=\begin{cases}s_n''(r) & 2\le n\le L\\ 0 & n>L\end{cases}\quad\text{and}\quad dc_n^*=\begin{cases}dc_n & 2\le n\le L\\ c_n & n>L\end{cases}.\tag{9c}$$

By differentiating Eq. (9b) with respect to the modification parameters $s_k''(r)$ and equating the result to zero and after further simplifications the corollary is proved.

Corollary 3 *The OLSM parameters* $s_n''(r)$ *are derived by considering* $b_n''(r)=\left\{\left[Q_n^L(r,\psi_0)\right]_{rr}+s_n''(r)\right\}c_n/(c_n+dc_n)$ *and solving the system of equations Eq. (2e) by considering*

$$h_k(r)=\Omega_k''(r)\sigma_k^2-\left[Q_k(r,\psi_0)\right]_{rr}d_k+\sum_{n=2}^{\infty}\left\{\left[Q_k(r,\psi_0)\right]_{rr}d_n-\Omega_n''(r)\sigma_n^2\right\}E_{nk}(\psi_0).$$

Proof. If the general error estimator Eq. (7) is written in the following spectral form:

$$\delta\tilde{T}_{rr}(P)=\frac{R}{4\pi}\iint_{\sigma_0}S_{rr}^{L}(r,\psi)\varepsilon^{\mathrm{T}}(Q)d\sigma+\frac{R}{2}\sum_{n=2}^{L}b_n''(r)\varepsilon_n^{\mathrm{EGM}}(P), \tag{10a}$$

then the spectral form of the above error estimator will be:

$$\delta\tilde{T}_{rr}(P)=\frac{R}{2}\sum_{n=2}^{\infty}\left\{\Omega_n''(r)-s_n''^{*}(r)-\left[Q_n^{L}(r,\psi_0)\right]_{rr}\right\}\varepsilon_n^{\mathrm{T}}(P)+\frac{R}{2}\sum_{n=2}^{M}b_n''(r)\varepsilon_n^{\mathrm{EGM}}(P). \tag{10b}$$

The global mean square error of the estimator is:

$$E\left\{\delta\tilde{T}_{rr}\right\}=\frac{R^2}{4}\sum_{n=2}^{\infty}\left\{\left[b_n''^{*}(r)-s_n''^{*}(r)-\left[Q_n^{L}(r,\psi_0)\right]_{rr}\right]^2c_n+\right.$$
$$\left.+\left[\Omega_n''(r)-s_n''^{*}(r)-\left[Q_n^{L}(r,\psi_0)\right]_{rr}\right]^2\sigma_n^2\right\}+\frac{R^2}{4}\sum_{n=2}^{M}b_n''^{2}(r)dc_n, \tag{10c}$$

Taking the derivative of Eq. (10c) with respect to $s_k''(r)$ and after further simplification the corollary is proved.

4 Numerical investigations

The EGM96 (Lemoine et al. 1998) is used to generate gravity anomaly and its error spectra. A correlation length of 0.1° and a standard error of 5 mGal are considered to generate the error spectra of terrestrial gravity anomaly. The EGM96 to degree and order M = 150 is used equal to the maximum degree of modification, L = 150. The BLSM, ULSM and OLSM methods are used to modify ESF and its SORD. The instability of Eq. (2e) to estimate the modification parameters in the ULSM and OLSM has been investigated by Ågren (2004), Ellmann (2004 and 2005). Here we take advantage of the truncated singular value decomposition method for regularizing Eq. (2e). According to Ellmann (2004) one can use any other regulator in this respect. Ågren (2004) also showed that the instability of this system of equations is harmless. The main goal of these studies was to modify Stokes' formula to determine a geoid. However, as was explained earlier, in order to construct a system of equations like Eq. (2e), to estimate the modification parameters, the derivative of global mean squares error of the estimator is taken with respect to $s_k(r)$ or $s_k''(r)$ (which are altitude-dependent) directly, which lead to the same coefficients matrix as that was obtained by Ågren (2004) and Ellmann (2005). Consequently, this matrix will have the same properties as that is used in modifying Stokes' formula and the conclusions made in these studies are also valid in our study. The important difference is due to the computation of the truncation coefficients and the spectra of ESF and/or its SORD.

Here, we consider two different approaches to generate T_{rr} at satellite level, either modifying the disturbing potential estimator, Eq. (2a) and after that taking the SORD of the modified estimator or modifying the T_{rr} estimator, Eq. (5a), directly. Obviously, these methods will not yield the same results, as the former method minimizes the global mean square error of the disturbing potential and not its SORD. However, we will investigate in which cases they yield similar results in practice.

This section consists of four parts. As was mentioned, the modification parameters and the truncation coefficients are altitude-dependent. Subsection 4.1 will consider this matter for ESF and its SORD. The modified ESK and its SORD are dependent on altitude, error spectral of the EGM or terrestrial data as well as the truncation error of the integral. Subsection 4.2 assumes a constant altitude and investigates different cases of modification based on the error spectra of the data in Methods 1 and 2. Also it will illustrate $b_n(r)$ and $b_n''(r)$ obtained from both methods with errorless and erroneous data. Subsection 4.3 presents the global root mean square error (RMSE) of Methods 1 and 2. Subsection 4.4 considers Fennoscandia as a test area to generate T_{rr}.

4.1 $b_n(r)$, $Q_n(r,\psi_0)$, $b_n''(r)$ and $\left[Q_n(r,\psi_0)\right]_{rr}$ at different altitudes

So far most of the geodesists worked on modification of Stokes' formula. In such a case the truncation coefficients of Stokes' kernel are not altitude-dependent and it is enough to generate the modification parameters once during the integration of Stokes' integral. In airborne gravimetry the truncation coefficients are altitude-dependent but the aircraft's height is restricted to few kilometers, say e.g. to 5 km, which is considerably lower than satellites' altitude. In this way of gravimetry the integration is performed after downward continuation of the airborne data. Few persons considered modification at airborne level; see e.g. Sjöberg and Eshagh (2009). If regeneration of the airborne data is required, one can estimate the truncation coefficients just once as the aircraft height is approximately constant. The situation at satellite level is complicated; firstly the altitude of a satellite is very large. Secondly due to very large orbital perturbations the satellite altitude cannot be regarded constant. Shepperd (1982) used a similar mathematical technique as used by Hagiwara (1978) to derive a recursive formula for generating the altitude-dependent truncation coefficients. He obtained the formula but it was impractical because of instabilities with respect to elevation (although his mathematical derivations were correct). Shepperd (1982) stated that this formula can work for the altitudes not higher than 20 km. Therefore one concludes that Shepperd's (1982) formula works for airborne gravimetry aspects. The other idea is to carry out a numerical integration process to solve the integral formula of the truncation coefficients, namely Eqs. (3c) or (6b). We numerically tested this matter and concluded the non-efficiency of this idea. Our studies showed that the integration error defects the result and increasing the integration step size would be very time consuming. One may use this method for the cases where the altitude is constant and the numerical integration should be performed once. However, this method should not be used in the ULSM and OLSM as the truncation coefficients are in the right

hand side of Eq. (2e); and since the coefficient matrix of this system of equations is unstable then the harmlessness condition of the instability of the system is not preserved. In this case, the estimated modification parameters are defected by the integration error of the truncation coefficients. After some tests, we concluded to use the spectral form of the truncation coefficients (Eqs. 3d and/or 6c), involving Paul's coefficients $e_{nn'}(\psi_0)$. The Paul's coefficients are not difficult to compute using the recursive formulas presented e.g. by Paul (1978). The only problem is that summation cannot be performed to infinity. We can select a large number (like 7000) as a truncation number. We tested and compared different truncation numbers for this series and we found that as long as the truncation number is above 5000 the truncation coefficients are more or less the same.

The truncation coefficients are altitude-dependent therefore the modification parameters will be altitude-dependent as well. If we look at Eqs. (2a) and (5a) we will find out that the second terms of both estimators which contribute the long wavelength structure of the estimators involve $b_n(r)$ or $b_n''(r)$ which are altitude-dependent as well (because of altitude-dependency of the truncation coefficients and the modification parameters).

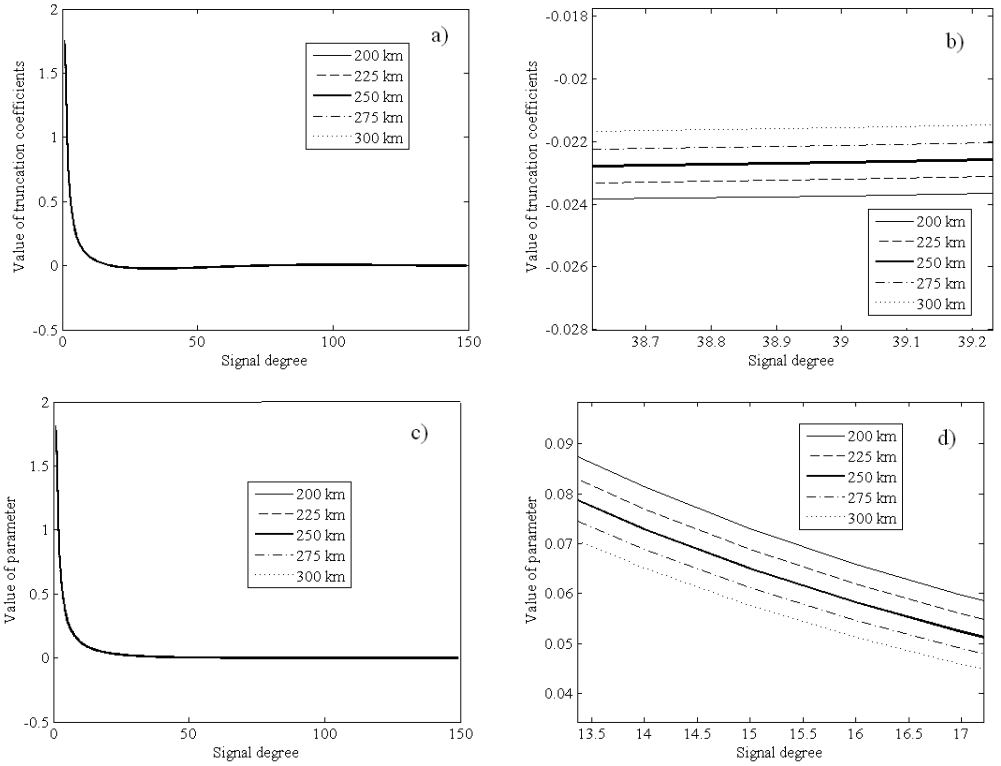

Fig. 1. a) and b) $Q_k(r,\psi_0)$ and c) and d) $b_n(r)$ at different altitudes, $L = 150$ and $\psi_0 = 3^\circ$

Figure 1 shows the truncation coefficients $Q_k(r,\psi_0)$ and $b_n(r)$ of Eq. (2a) at different altitudes. Since the plots are very close only one curve is visible in Figs. (1a) and (1c). However, we have selected and zoomed one part of each figure and

presented them in Figs. (1b) and (1d). Figures (1c) and (1d) are $b_n(r)$ for the BLSM. Because of having very similar plots for the ULSM and the OLSM we did not present their $b_n(r)$. However, the consequence of their presentation will be the same as that of the BLSM. Figure (1b) which is a zoomed part of Fig. (1a), shows that the magnitude of truncation coefficients and modification parameters decreases by increasing altitude.

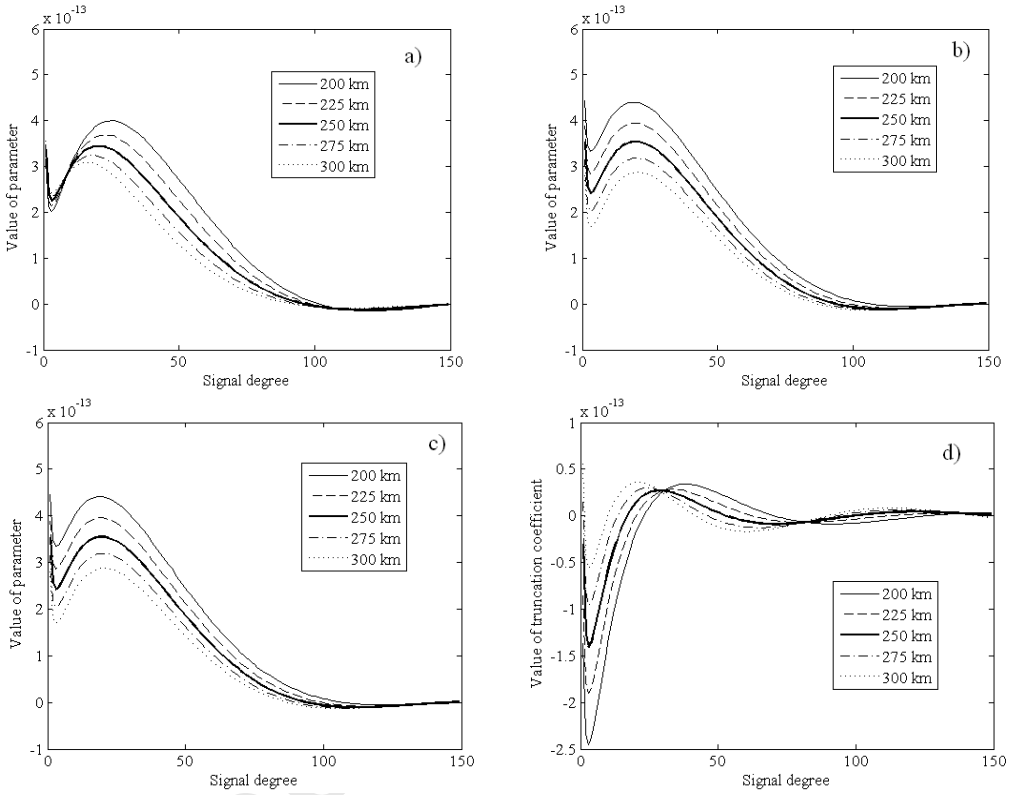

Fig. 2. $b_n''(r)$ in a) BLSM, b) ULSM and c) OLSM, d) $\left[Q_k(r,\psi_0)\right]_{rr}$ at different altitudes, $L = 150$ and $\psi_0 = 3^\circ$

Figures (2a), (2b) and (2c) show the parameter $b_n''(r)$ of the T_{rr} estimator modified by the BLSM, ULSM and OLSM, respectively at different altitudes. Figure (2d) is the truncation coefficient $\left[Q_k(r,\psi_0)\right]_{rr}$. As the figure illustrates the truncation coefficients frequently change with degrees. Its magnitude is smaller than the others at altitude 300 km to the degrees lower than 40 and larger to the degrees around 80 and so on. The reverse situation is observed for the altitude 200 km. It is different from the truncation coefficients of the disturbing potential which has a decreasing pattern. Figures (2b) and (2c) are very similar and they show the parameter $b_n''(r)$ based on the ULSM and OLSM. The value of the parameter is smaller for the altitude 300 km than those with lower altitude. Figure (2a) differs with these two figures as it has similar pattern after the degree around 15. Before this degree it has the reverse situation. We know that the modification parameters are obtained through

the solution of an ill-conditioned system of equations in the ULSM and OLSM. Such a system of equations is solved by the truncated singular value decomposition method which is a smoothing solver. Smoothness of the solution of the modification parameters might be the reason of the differences between $b_n''(r)$ in the BLSM and the ULSM or OLSM.

4.2 Modified SORD of ESK and $b_n''(r)$ in Methods 1 and 2

The modification parameters are the main factors for the changes in ESK. As was already explained these parameters are estimated in such way that ESK gets close to zero at the end of the cap size of integration, or in other words, it becomes sensitive to the existing data around the computation point. Effectiveness of modification can be presented by plotting the original and modified ESK in different geocentric angles in one plot. It should be reminded that Method 1 (taking derivative before modification) and Method 2 (modification before taking derivative) are considered in this subsection. Similar to the numerical studies performed in previous subsections the maximum degree of modification is L = 150 and the cap size of integration is 3°. Figures (3a), (3b) and (3c) show the modified ESK by Method 1 with the BLSM, ULSM and OLSM, respectively. In these figures different cases for the LSM are considered. First we assume that there is no error neither in terrestrial data ($\sigma_n^2 = 0$) nor in the EGM based data ($dc_n = 0$). It means that we 100% rely on the quality of the data. Therefore the only error to minimize will be the truncation error of the SORD of ESF. In the second case, we consider these errors in the LSM. The third case considers no error in terrestrial data and the last case no error in the EGM data. The same situation holds for Method 2 in Figs. (3b), (3d) and (3f). Figures (3a), (3c) and (3c) express that the LSM is feasible and meaningfull in all cases. As Figs. (3b), (3d) and (3f) represent in some cases Method 2 works and in some does not. This method does not work when only the EGM error is considered. It is natural because we assumed that the terrestrial data are errorless then the estimator considers very high weight for them. By taking the SORD, the error of the EGM data is amplified; on the other hand, the estimator is subjected to errorless terrestrial data and concentrates on the data which contains a small portion of the gravitational signal (high frequency). Consequently, the ESK has to change largely to fulfill this constraint.

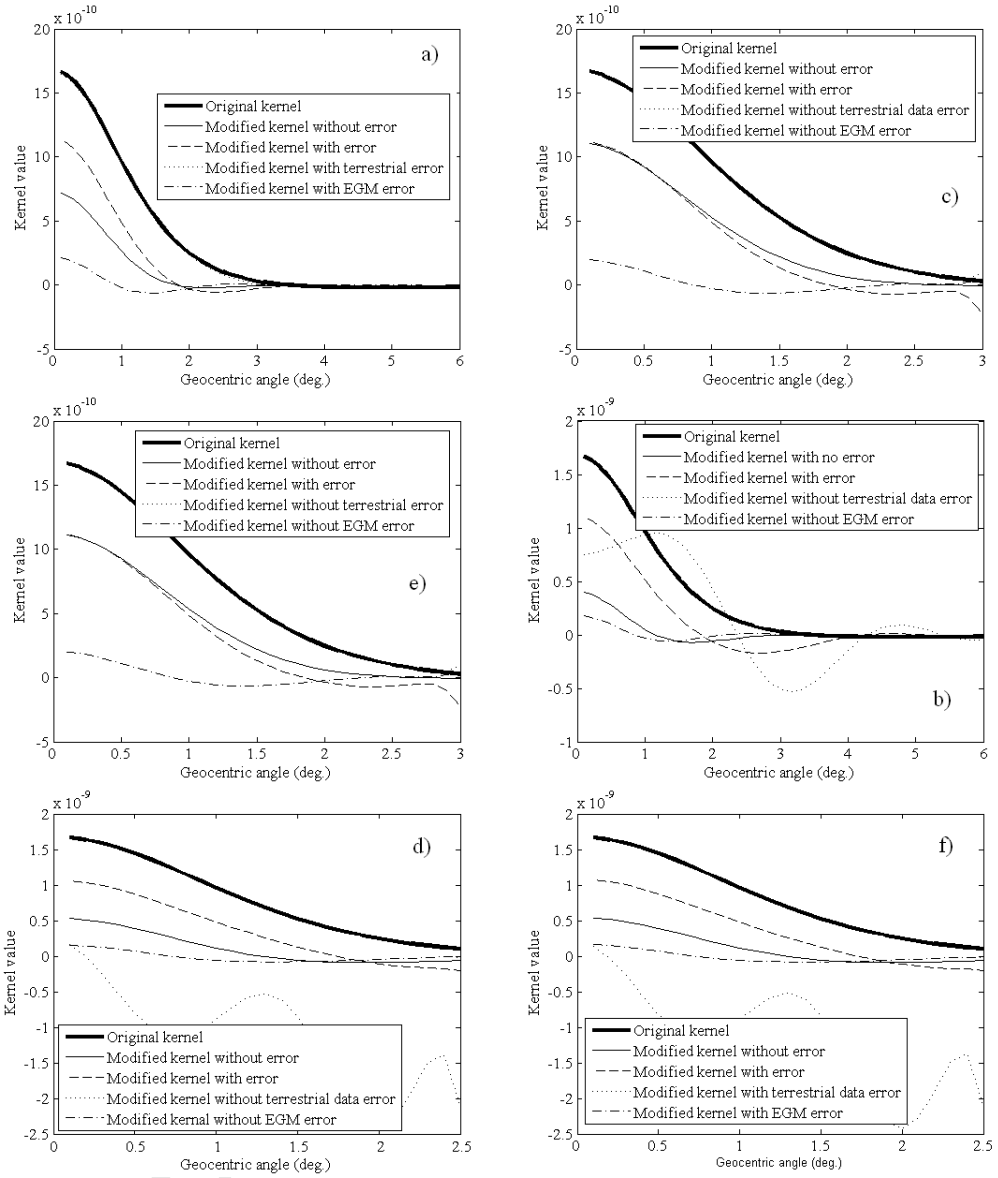

Fig. 3. a), c) and e) modified ESK by Method 1 using BLSM, ULSM and OLSM, respectively, b), d) and f) corresponding modified ESK by Method 2, $L = 150$ and $\psi_0 = 3^\circ$

ESK and the involved integral are responsible of recovering the high frequencies of the gravitational signal. The low frequencies are recovered using the second terms of the estimators Eqs. (2a) and (5a) involving $b_n''(r)$. These parameters are depicted in Fig. 4. This figure shows $b_n''(r)$ obtained based on Methods 1 and 2 with errorless and/or erroneous data. The parameters $b_n''(r)$ which are based on the modified estimator by the ULSM and OLSM have very similar patterns, but Fig. (4a) shows slightly different $b_n''(r)$ related to the BLSM with respect to the other LSM methods.

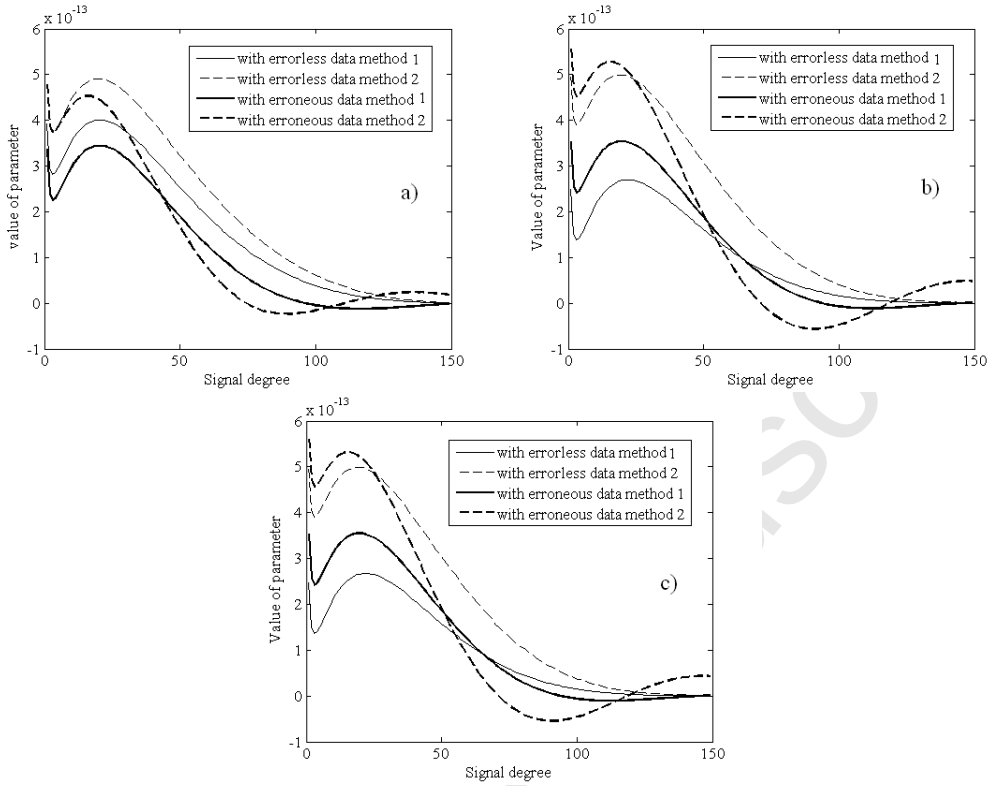

Fig. 4. $b_n''(r)$ obtained by Methods 1 and 2 based on, a) BLSM, b) ULSM and c) OLSM

4.3 Methods 1 and 2 in a global RMSE point of view

Equations (2a) and (5a), or ESF and its SORD are modified in a least-squares sense, which means that the modification parameters are estimated in such a way that the global RMSE of the estimators is minimized. Substituting the estimated modification parameters into the mathematical expression of the global RMSE yields the global RMSE of each estimator. This error can be a criterion to judge about quality of the LSM and Methods 1 and 2.

Figures (5a) and (5b) show the global RMSE of Eq. (2e) with and without error of data. We present these figures to show that the global RMSE of the estimator is decreasing with increasing the cap size of modification (as it is expected). Figures (5c) and (5e) represent the global RMSE of the estimator Eq. (5a), which is the SORD of ESF, or in other words, Method 1. Similar pattern is observed for both cases in which the error of data is included or excluded. The errors are also decreasing by the increasing the cap size of modification. It is also reasonable as by adding more data in least-squares estimation the errors decay. Method 2 is the case that ESF is modified using the LSM methods and after taking the SORD of modified ESF the errors are estimated. Figure (5d) illustrates that when the SORD of the modification parameters in inserted to the mathematical formula of the global RMSE of the SORD of ESF the errors are still decreasing. Since we observed large variations in the errors we had to plot the vertical axis of the errors in logarithmic

scale for better visualization. As can be seen in the figure, the errors are considerably large before the geocentric angle 2.5° for the modified estimators by the ULSM and OLSM with Method 2, while the error of the BLSM remains smaller than 0.01 E to the cap size 10°. The consequence of considering no error for the data will be similar. The main important conclusion that can be made here is related to the proper choice of cap size of modification in Method 2. One should be very careful to select the cap size prior to using this method; otherwise the method will yield wrong results. Figures (5d) and (5f) show that Method 2 works as long as the cap size is larger than 2.5° for the modified estimator by the ULSM and OLSM. Method 2 will work without problem for the BLSM case.

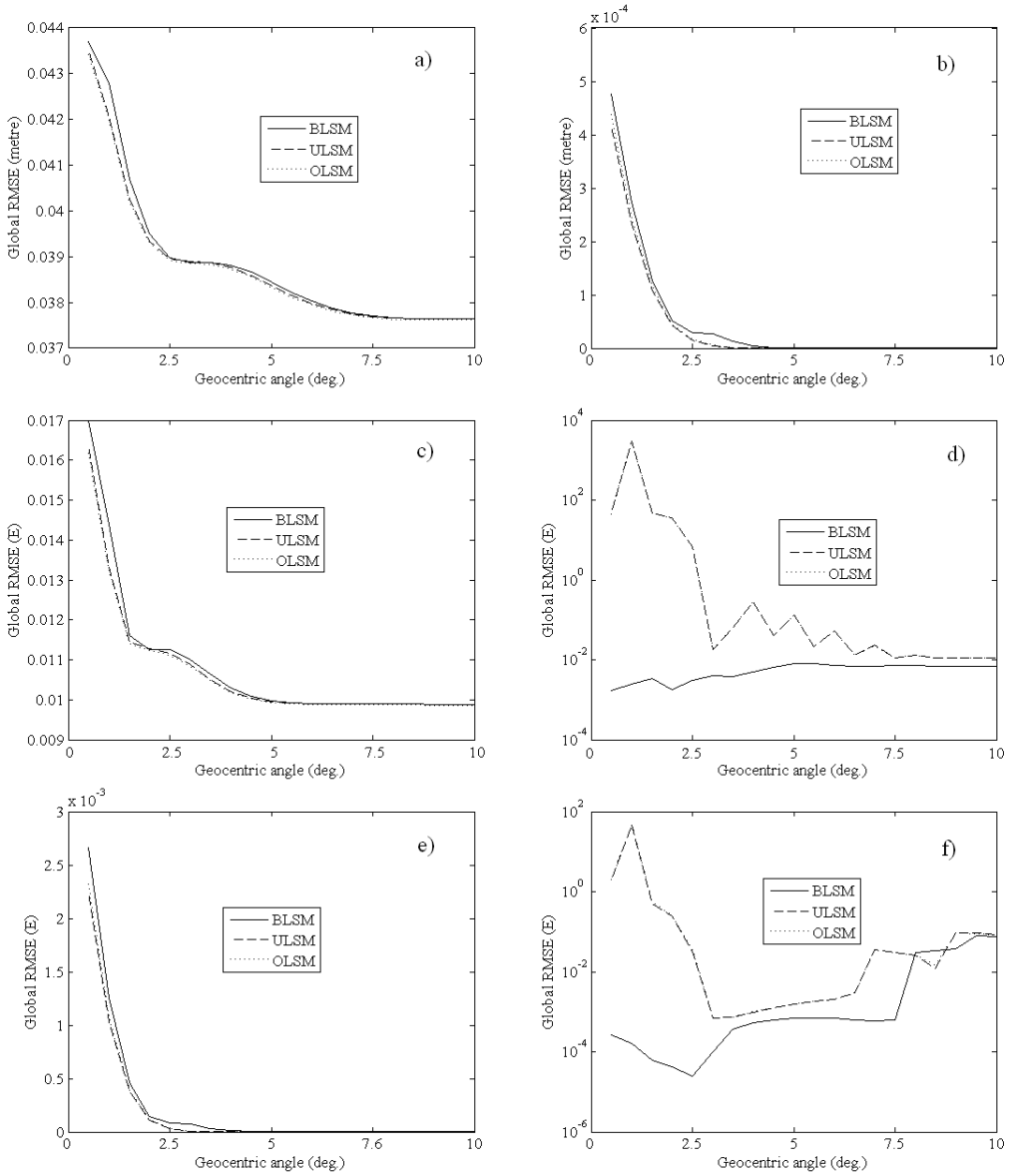

Fig. 5. Global RMSE of a) disturbing potential with erroneous data, b) with errorless data, of c) T_{rr} with erroneous data Method 1, d) T_{rr} with erroneous data Method 2, e) T_{rr} with errorless data Method 1, f) T_{rr} with errorless data Method 2.

4.4 Generation of T_{rr} over Fennoscandia by Methods 1 and 2

As was explained in the introduction of this section, the EGM96 is assumed as the true gravitational field. A regular grid of gravity anomalies were generated with the $30' \times 30'$ resolution and the goal is to estimate T_{rr} at 250 km level. Methods 1 and 2 are tested in different cap sizes of integration, resolutions of the terrestrial data, error of the terrestrial and the EGM data and the degree of modification. Fennoscandia limited between latitudes 50° and 75° and longitudes 0° and 35° is selected as the test region. T_{rr} is generated in a grid with the same resolution of the gravity anomalies at sea level using Methods 1 and 2 and the LSM techniques. The statistics of the gravity anomalies and T_{rr} are presented of the test area in Table 1. Gravity anomalies have more or less a smooth pattern in Fennoscandia. The maximum and minimum of the anomalies are situated in the Norwegian mountains and in the middle of Baltic Sea, respectively. The maximum and minimum of T_{rr} are also in these two regions. Figure 6 shows the maps of the anomalies and T_{rr} in Fennoscandia.

Table 1. Statistics of gravity anomalies and T_{rr} in Fennoscandia

	Max	Mean	Min	Std
T_{rr} (E)	0.430	-0.002	-0.455	0.187
Δg (mGal)	73.844	3.582	-54.643	17.284

Having a general view of the regime of the gravity anomaly and the gradient T_{rr}, we continue the studies on modification and estimation of the gradients over this region.

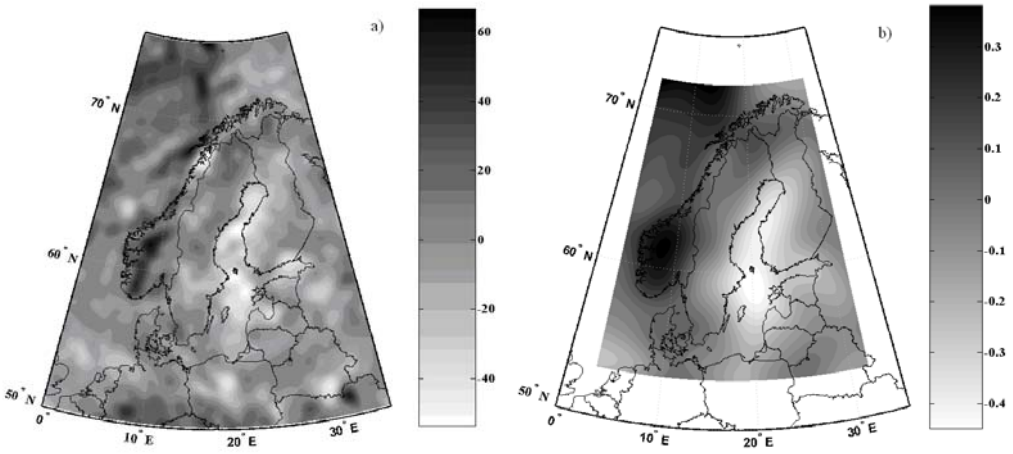

Fig. 6. a) Gravity anomalies (mGal) and b) T_{rr} (E) in Fennoscandia

4.4.1 Test of cap size of modification

The gradient T_{rr} is generated directly from the EGM96 and is supposed to be the true gradient. This gradient is also generated using Methods 1 and 2. The numbers " 1 " and " 2 " in the tables of this section deal with these two methods. The generated gradients using these methods are compared with that were obtained directly from the EGM96 and the statistics of their differences (the errors of T_{rr}) are presented. Two cases are considered in all parts of the numerical studies, where the errorless and erroneous data are used in the LSM of ESF and its SORD. Table 2 shows the statistics of the errors of T_{rr} for the caps sizes 3° and 2°. As the table shows when Method 1 is used and the errors of the data are set to zero, the BLSM yields the gradient with an error of 2 mE, while the ULSM and the OLSM do with a 13 mE error which is 6 times larger. If the cap size of modification reduces to 2° the BLSM's error reaches to 10 mE but error of the other LSMs is larger (35 times). Now let us consider Method 2. As we see in the table, this method can somehow estimate the gradient. If the BLSM is used, the error is 4 mE and it is roughly about 12 mE (three times larger) for the other LSM methods. By selecting a cap size of 2°, the ULSM and OLSM do not perform well and the errors are unrealistically large, while the BLSM still works with 6 mE error. If we return to Method 1 and include the data errors in the LSM, the error will be 4.6 mE for the BLSM and 7 mE for the ULSM and OLSM. The interesting issue is the improvement achieved by including the data error. When we consider zero error for the data, the estimator consider the same and very high weights for the data in the cap size and the EGM based data. However, when we add some errors to the terrestrial data, the errors are balanced in the LSM and the terrestrial data contributes according to their accuracies. One may ask why the BLSM based estimator was not improved. Actually existence of $Q_n^L(r,\psi_0)$ in $b_n''(r)$ increases the sensitivity of the estimator to the cap size in the ULSM and OLSM. In other words, some properties of the integral part of the estimator contribute to the second part, while this is not the case for the BLSM. In fact by reducing the weight of the data in the cap size of the integration the solution goes closer to that gradient obtained directly from the EGM and this is why we see better results in these two cases in the presence of the data errors. As we observe Method 2 does not work when the cap size is 2° and the sign " ! " we putted in the table means very big and unrealistic number which are due to weakness of the method in this cap size. In the case of using a cap size of 3° Method 2 works with an error of about 0.05 E.

Now let us select a cap size of 2.5°. Table 2 shows the results of integration based on this cap size. Method 1 with errorless data yield 10 mE error based on BLSM and 20 mE based on the others. Method 2 yields 7 mE error with the BLSM while for the ULSM and OLSM is about 150 mE. In the case of including the data error again Method 1 with the BLSM seems to work with an error of 11 mE. Method 2 yields large errors when the ULSM and OLSM are used. We putted the sign " ! " instead of the very large numbers in the table. Methods 1 and 2, including the data error, yield the gradients with errors of 11 mE and 50 mE, respectively.

Table 2. Statistics of errors of T_{rr} for the cap sizes $\psi_0 = 3^\circ$ and 2° with $30' \times 30'$ resolution for the gravity anomalies and gradient and with L=150. Unit : 1 mE

			$\psi_0 = 3^\circ$				$\psi_0 = 2^\circ$			
			Max	Mean	Min	Std	Max	Mean	Min	Std
Errorless data	1	BLSM	4.2	-0.4	-11.6	**2.2**	13.7	-3.1	-46.9	10.3
		ULSM	14.6	-3.9	-60.7	12.7	689.4	-96.1	-999.5	349.2
		OLSM	14.7	-3.9	-61.5	13.0	710.0	-100.3	-1041.0	364.2
	2	BLSM	17.6	1.4	-7.2	**4.0**	19.1	1.5	-13.9	**6.1**
		ULSM	40.2	3.2	-19.6	11.1	3309.5	319.2	-2433.0	1200.5
		OLSM	41.6	3.3	-21.5	11.6	3504.6	337.9	-2545.9	1268.2
Erroneous data	1	BLSM	13.2	-0.2	-12.4	**4.6**	25.0	-6.0	-88.8	20.0
		ULSM	22.9	1.0	-17.8	7.5	2469.0	241.8	-1788.7	892.5
		OLSM	23.3	1.0	-18.2	7.6	2406.4	235.8	-1721.7	868.2
	2	BLSM	125.8	9.2	-85.4	41.6	163.0	12.8	-154.3	64.1
		ULSM	176.9	12.5	-112.7	55.1	**!**	**!**	**!**	**!**
		OLSM	178.3	12.8	-113.1	55.8	**!**	**!**	**!**	**!**

Table 3. Statistics of error of T_{rr} for the cap size $\psi_0 = 2.5^\circ$ with $30' \times 30'$ resolution for the gravity anomalies and gradient with L=150. Unit: 1 mE

			$\psi_0 = 2.5^\circ$			
			Max	Mean	Min	Std
Errorless data	1	BLSM	13.1	-3.1	-50.1	10.3
		ULSM	33.1	-6.2	-83.3	21.3
		OLSM	33.3	-6.3	-85.3	21.9
	2	BLSM	22.9	1.9	-13.6	**6.72**
		ULSM	401.3	34.7	-287.4	144.3
		OLSM	424.5	36.9	-303.4	153.2
Erroneous data	1	BLSM	15.9	-3.6	-56.2	10.7
		ULSM	14132.2	117.7	1004.6	502.3
		OLSM	1388.4	117.0	-985.6	497.8
	2	BLSM	148.0	11.0	-147.8	52.4
		ULSM	**!**	**!**	**!**	**!**
		OLSM	**!**	**!**	**!**	**!**

One consequence of this section is that a cap size of 3° is suitable for integrating the terrestrial data. Selection of larger cap size will not be interesting. As Fig. 5 shows the SORD of ESK is very close to zero for larger geocentric angles and modification with such a cap size is not appropriate. Eshagh (2009) studied the meaningfulness of the modification with a 3° cap size and found 0.1 E difference between the cases where the formula is modified and is not modified. We can learn from Tables 2 and 3 that Method 2 will work if we rely 100% on the quality of the existing data. In this case the LSM methods perform like the deterministic methods in which just the truncation error of the formula is minimized. Eshagh (2009) has also compared the Molodensky's modification (Molodensky et al. 1962) and compared it with the BLSM and found very similar results. Since errorless data is considered in the LSM of ESF then taking SORD, which acts as an amplifier operator, will not change the estimate significantly as there is no data error to be amplified. The BLSM seems to be the most suitable

method for generating the gradient at satellite level. It seems smoother LSM than the others. Although the differences between these methods may not be significant theoretically but practically they are as we can see most of the friends of the LSM methods use the ULSM (Ågren 2004) or OLSM (Ellmann 2005, Kiamehr 2006, Daras 2008 and Abdallah 2009) in modifying Stokes' formula for geoid determination. The reason could be the sensitivity of these LSM methods to the terrestrial data which are responsible to recover high frequencies of the geoid. As we showed in Table 3 Method 2 can generate the gradient with a 6 mE error which is smaller than that is estimated by Method 1 (10 mE). It should be mentioned that proper regularization of the system of equations Eq. (2e) in ULSM and OLSM is not meaningful as the instability of the system is harmless and the differences are not due to regularization. It is also similar to the results of Wolf (2007) who concluded that the caps size 2.5° is the best. As it is clear from her thesis, she used the deterministic approaches and the spectral weighting scheme in her computations which is in agreement with Method 2 with the BLSM and with errorless data.

4.4.2 Test of resolution and error of terrestrial data

In order to investigate the dependence of Methods 1 and 2 to the terrestrial data we consider one test on the resolution and another on the error of terrestrial and the EGM data. Table 4 shows the statistics of the errors of the estimated T_{rr} by Methods 1 and 2 with the resolution $15'\times15'$ and with errorless and erroneous data. Insignificant changes are observed in the table, as there is no information higher than the nyquist frequency of the EGM96. The resolution of this EGM is $30'\times30'$ corresponding to degree and order 360. Consequently, the enhancement of the results (if any) will be very small as the attenuation factor reduces higher frequencies at satellite level. Clearly, if an EGM with higher resolution is used the data with higher resolution may not be used. In the second part of our investigation, we work with the $30'\times30'$ data and test the influence of the error of terrestrial data. At first, we consider no error in the EGM based data namely dc_n =0 and modify the estimators assuming 5 mGal error in terrestrial data. That part of the table which is related to this study is separated by σ_n^2 meaning that there is terrestrial data error in the LSM. We see very considerable reduction in the error of the estimated gradients. As we see Methods 1 and 2 yield the same error of 2 mE and the error of Method 1 based on ULSM and OLSM is about 3 mE. Such a good result could be expected as by including the error of the terrestrial data in the LSM process the terrestrial data are down-weighted and the methods yield closer results to that gradient directly obtained from the EGM. Reversely, if we consider no error in the terrestrial data and up-weight the data, the contribution of the EGM is reduced. Since the long wavelength structure of the gravitational field has the major contribution in satellite data, therefore putting high weights for a small portion of data, which are restricted to a certain cap size, cannot estimate the gradient well at satellite level. This is why we observe large errors for Method 1 with erroneous data. The situation will be even worse for Method 2 as the errors are considerably amplified by taking SORD. This subsection shows the importance of the quality of the EGM which is used.

Table 4. Statistics of errors of T_{rr} for testing resolution and error of terrestrial data in Methods 1 and 2 for $\psi_0 = 3^\circ$ and L =150. Unit: 1 mE

			$15' \times 15'$				$30' \times 30'$				
			Max	Mean	Min	Std	Max	Mean	Min	Std	
Errorless data	1	BLSM	4.5	-0.5	-13.5	**2.5**	6.0	0.5	-6.3	**2.1**	σ_n^2
		ULSM	17.0	-4.0	-64.8	13.6	6.8	0.17	-8.0	**2.8**	
		OLSM	16.7	-4.1	-65.7	13.9	9.5	0.3	-9.4	**3.3**	
	2	BLSM	18.0	1.4	-7.6	**4.2**	6.0	0.5	-6.3	**2.1**	
		ULSM	39.7	3.0	-21.0	11.3	71.8	5.7	-39.9	20.8	
		OLSM	41.0	3.0	-22.9	11.8	74.3	6.1	-43.1	22.3	
Erroneous data	1	BLSM	13.8	-0.5	-14.9	**4.6**	50.4	-11.3	-165.6	37.6	dc_n
		ULSM	20.8	0.5	-18.4	**7.1**	55.2	-12.2	-175.9	40.6	
		OLSM	21.3	0.6	-18.8	**7.3**	55.2	-12.2	-175.9	40.6	
	2	BLSM	122.2	8.2	-88.4	40.6	335.8	18.3	-263.2	110.1	
		ULSM	167.4	10.7	-108.6	52.0	**!**	**!**	**!**	**!**	
		OLSM	168.9	10.9	-109.0	52.6	**!**	**!**	**!**	**!**	

4.4.3 Test of degree of modification

Degree of modification shows the contribution of the long wavelength structure of the EGM used in the LSM. Here we consider four degrees of modification 100, 125, 175 and 200. We already investigated the degree 150 in the previous subsections. Table 5 shows the statistics of the errors of T_{rr} estimated by Methods 1 and 2 with degrees of modification of 100 and 125. When L = 100 we see large error for Method 1 and in the same order as that is for all the LSM methods considering errorless data. Method 2 delivers the error in the same level of Method 1 for BLSM, but the errors are twice larger for the others. When the errors of the data are included, Method 1 performs better with an error of 5 mE for all the LSM methods. However, the errors of Method 2 are considerably larger than that of Method 1. If the degree of modification increases to 125 the results seem better in Method 1 with errorless data. Method 2 is good just with the BLSM. Method 1 with the BLSM and in the presence of erroneous data performs similarly with an error of 7 mE. As was explained before, the ULSM and OLSM are more sensitive to the terrestrial data than the BLSM and when the degree of modification, or in other words, the EGM contributes further and Method 1 using the BLSM yields smaller error, while when higher degrees of the EGM are included the their errors are cumulatively increased as well.

Table 6 is similar to Table 5 but for the modification degrees 175 and 200. Some improvements are seen in the estimated T_{rr}. Method 1 yields T_{rr} with a 2.7 mE error based on the BLSM and 9 mE based on the ULSM and OLSM when the data are errorless and L = 175. If such errorless data are considered for Method 2 the errors of the method will be 1.8 mE for the BLSM and 8 mE for the others. If the degree of modification increases to 200 we will not see significant improvement in the methods with the BLSM, but the errors will be reduced by about 2 mE for the ULSM

and OLSM. Similar results can be achieved if the erroneous data are considered in the modification, but the error of the method will increase by about 2 mE. The other LSMs will improve the estimation about 1 mE. The error of Method 2, in the presence of the erroneous data, is about 42.0 mE for the L = 175 and L = 200, which means that after a certain degree Method 1 based on the BLSM will not improve the estimation. However, this is not the case for the ULSM and OLSM as very significant differences are observed in the errors. The error of Method 2 is about 14 mE when L =175 while it is 178 mE when L =200. This error is 8.6 mE in the former case while it is 212 mE in the latter. One can conclude that it is possible to find an optimum degree of modification for the ULSM and OLSM. Therefore, we can expect to find such a degree for Method 2 based on the ULSM and BLSM if the modification degree is properly selected. We have further investigated Method 2 at different degrees of modification. We found that the minimum achievable error using Method 2 and the ULSM is 11.8 ~ 12 mE at L = 170 and 6.6 ~ 7 mE around L = 189 for the OLSM.

Table 5. Statistics of errors of T_{rr} estimated based on Methods 1 and 2 for $\psi_0 = 3^\circ$ and resolution $30' \times 30'$. Unit : 1 mE

			L=100				L=125			
			Max	Mean	Min	Std	Max	Mean	Min	Std
Errorless data	1	BLSM	26.7	-6.7	-100.6	**21.7**	14.37	-3.9	-62.3	12.8
		ULSM	30.5	-7.5	-110.7	24.2	20.9	-5.4	-82.7	17.6
		OLSM	30.9	-7.5	-112.0	24.6	20.92	-5.5	-83.8	17.9
	2	BLSM	67.9	5.4	-40.1	**21.8**	40.9	3.3	-21.7	11.9
		ULSM	180.8	13.2	-102.5	53.4	107.6	8.1	-56.7	31.5
		OLSM	190.9	14.0	-108.4	56.3	113.2	8.6	-60.3	33.1
Erroneous data	1	BLSM	10.0	-1.2	-23.1	**4.2**	11.64	-0.9	-18.9	**4.0**
		ULSM	16.2	0.1	-13.3	**5.1**	21.1	0.7	-16.6	**6.9**
		OLSM	16.4	0.2	-13.9	**5.4**	21.1	0.7	-16.7	**6.9**
	2	BLSM	117.4	9.2	-79.9	40.3	122.3	9.4	-80.0	41.3
		ULSM	523.7	37.5	-304.6	153.7	1.0 E	76.7	-547.7	307.7
		OLSM	538.2	38.7	-310.6	158.0	1.0 E	75.0	-531.4	299.7

Table 6. Statistics of errors of T_{rr} estimated based on Methods 1 and 2 for $\psi_0 = 3^\circ$ and resolution $30' \times 30'$. Unit: 1 mE

			L = 175				L = 200			
			Max	Mean	Min	Std	Max	Mean	Min	Std
Errorless data	1	BLSM	11.0	1.0	-5.2	**2.7**	8.9	0.8	-4.0	**2.1**
		ULSM	10.5	-2.8	-44.4	**9.2**	7.9	-1.9	-32.4	**6.8**
		OLSM	10.7	-2.8	-44.9	**9.4**	9.1	-1.9	-32.1	**7.0**
	2	BLSM	5.3	0.5	-5.2	**1.8**	5.2	0.2	-4.4	**1.8**
		ULSM	29.8	2.4	-12.6	**7.7**	22.5	1.8	-8.5	**5.6**
		OLSM	31.1	2.5	-14.5	**8.3**	23.9	1.9	-11.1	**6.3**
Erroneous data	1	BLSM	15.1	-0.1	-14.3	**5.2**	18.9	0.2	-19.5	**6.8**
		ULSM	27.8	1.1	-21.1	**8.9**	29.5	1.2	-24.1	**9.6**
		OLSM	27.8	1.2	-21.3	**8.9**	30.0	1.3	-24.7	**9.8**
	2	BLSM	129.7	8.9	-83.6	42.0	130.8	8.9	-84.4	42.0
		ULSM	44.9	1.7	-35.7	**14.0**	305.7	-46.1	-616.4	177.9
		OLSM	14.4	-2.8	-44.4	**8.6**	362.8	-54.9	-733.6	212.1

Although Method 1 yields good results in most cases but the main important assumption of this method is the isotropy of ESK. In this study we used the SORD of ESF because in the both methods we have isotropic kernels and possibility of comparing the methods. Method 2 works in special cases and one should be careful in the use of this method. Selection of the proper cap size and degree of modification is very important in this method. If these parameters are selected correctly Method 2 can be used for generating the gradient with error within 0.01 E. This method can also be used in generating the other elements of the tensor of gravitation.

5 Conclusions

In this paper the LSM methods were used for ESF and its SORD to generate T_{rr} at 250 km level. The mathematical formulas of elements of the system of equations from which the modification parameters are obtained based on the LSM methods were developed. We have shown that if we organize the system of equations in such a way that the altitude-dependent modification parameters and/or its SORD are directly solved the properties of the system of equations is the same as that is for the LSM of ordinary Stokes' formula for geoid computation. Two methods were presented to generate T_{rr} which were named Methods 1 and 2. Method 1 seems working very well depending on the accuracy of the data proper choice of the cap size of the integration and degree of modification. This method produced the best results when the degree of modification is $L = 150$ and the resolution of data is $30' \times 30'$ in a cap size 3° and if we consider an error-free EGM. Definitely by increasing the degree of modification better results would be achieved. Method 2 is very sensitive to proper choice of these parameters otherwise the results will be wrong. The reason is the amplification of the errors by taking SORD from the modified ESF. In this study we found that if the cap size of integration is around 3° and the degree of modification is about 175 we can generate T_{rr} with 7 mE error using the ULSM and OLSM. If we assume no error in the LSM except the truncation error of ESF, Method 2 with the BLSM will work with sufficient accuracy. This method is very similar to deterministic modification and therefore we can conclude Method 2 with a deterministic modifier should work.

Acknowledgements

The author would like to appreciate Professor Lars E. Sjöberg for the scientific discussion about least-squares modification. The Swedish National Space Board (SNSB) is cordially acknowledged for the financial support, project no. 63/07:1. Mr. Mohammad Bagherbandi is appreciated for his criticisms on the draft version of the paper. Professor Randell Stephenson and his reviewing board are acknowledged.

List of abbreviations

Biased least-squares modification……....BLSM
Earth's gravitational model……EGM

Extended Stokes' function……...ESF
Extended Stokes' kernel……..ESK
Least-squares modification……LSM
Optimum least-squares modification ……..…OLSM
Root mean square error……RMSE
Satellite gravity gradiometry……..SGG
Second-order radial derivative……SORD
Unbiased least-squares modification……..…ULSM

References

Abdallah A. (2009) Determination of a gravimetric geoid model of Sudan using the KTH method. M.sc. Thesis in Geodesy and Geoinformatics Engineering, Royal Institute of Technology, Stockholm, Sweden.

Bouman J. and Koop R. (2003) Error assessment of GOCE SGG data using along track interpolation, Adv. Geosc. 1:27-32.

Bouman J., Koop R., Haagmans R., Muller J., Sneeuw N. Tscherning C.C., and Visser P.(2003) Calibration and validation of GOCE gravity gradients, Paper presented at IUGG meeting, pp. 1-6

Bouman J., Koop R., Tscherning C. C. and Visser P. (2004) Calibration of GOCE SGG data using high-low STT, terrestrial gravity data and global gravity field models, J Geod. 78:124-137.

Daras I. (2008) Determination of a gravimetric geoid model of Greece using the method of KTH, M.sc. Thesis in Geodesy and Geoinformatics Engineering, Royal Institute of Technology, Stockholm, Sweden.

Denker H. (2002) Computation of gravity gradients for Europe for calibration/validation of GOCE data, In Proc. IAG International symposium "Gravity and Geoid" Tziavos I.N. (ed.) Aug. 26-30, 2002, Thessaloniki, Greece, p.287-292.

Ellmann A. (2004) The geoid for the Baltic countries determined by the least squares modification of Stokes' formula, Doctoral thesis in Geodesy, Royal Institute of Technology, Stockholm, Sweden.

Ellmann A. (2005) Computation of three stochastic modification of Stokes' formula for regional geoid determination, Comp. & Geos. 31:742-755.

Eshagh M. (2009) On satellite gravity gradiometry, Doctoral thesis in Geodesy, Royal Institute of Technology, Stockholm, Sweden.

Haagmans R. Prijatna K. and Omang O. (2002) An alternative concept for validation of GOCE gradiometry results based on regional gravity, In Proc. Gravity and Geoid 2002, GG2002, August 26-30, Thessaloniki, Greece.

Hagiwara Y. (1972) Truncation error formulas for the geoidal height and the deflection of the vertical, Bull. Geod. 106:453-466.

Heiskanen W. and Moritz H. (1967) Physical Geodesy. W.H Freeman and company, San Fransisco and London.

Kaula W. (1963) The investigation of the gravitational fields of the moon and planet with artificial satellites. Adv. Space Sci. and Tech. 5:210-226.

Kiamehr R. (2006) Precise gravimetric geoid model for Iran based on GRACE and SRTM data and the least-squares modification of Stokes' formula with some geodynamic interpretations, Doctoral thesis in Geodesy, Royal Institute of Technology, Stockholm, Sweden

Kern M. and Haagmans R. (2004) Determination of gravity gradients from terrestrial gravity data for calibration and validation of gradiometric GOCE data, In Proc. Gravity, Geoid and Space missions, GGSM 2004, IAG International symposium, Portugal, August 30- September 3, pp. 95-100.

Kern M., Preimesberger T., Allesch M., Pail. R., Bouman J. and Koop R. (2005) Outlier detection algorithms and their performance in GOCE gravity field processing, J Geod. 78:509-519.

Lemoine F.G., Kenyon S.C., Factor J.K., Trimmer R.G., Pavlis N.K., Chinn D., Cox CM., Klosko S.M., Luthcke S.B., Torrence M.H., Wang Y.M., Williamson R.G., Pavlis E.C., Rapp R.H. and Olson T.R. (1998) Geopotential model EGM96. NASA/TP-1998-206861. Goddard Space Flight Center, Greenbelt.

Molodensky M.S., Eremeev V.F. and Yurkina M.I. (1962) Methods for study of the external gravity field and figure of the Earth. Trans. From Russian (1960), Israel program for scientific translation, Jerusalem.

Mueller J., Denker H., Jarecki F. and Wolf K.I. (2004) Computation of calibration gradients and methods for in-orbit validation of gradiometric GOCE data, In Proc. Second international GOCE user workshop "Goce, The Geoid and Oceanography", ESA-ESRIN, Frascati, Italy, 8-10 March 2004.

Pail R. (2003) Local gravity field continuation for the purpose of in-orbit calibration of GOCE SGG observations, Adv. Geosc. 1: 11–18

Paul M.K. (1978) Recurrence relations for integrals of associated Legendre functions, Bull. Geod. 52:177-190.

Reed G.B. (1973) Application of kinematical geodesy for determining the shorts wavelength component of the gravity field by satellite gradiometry, Ohio state University, Dept. of Geod Science, Rep. No. 201, Columbus, Ohio.

Shepperd S. W. (1982) A recursive algorithm for evaluating Molodeski-type truncation error coefficients at altitude, Bull. Geod. 56: 95-105.

Sjöberg L.E. (1980) Least-squares combination of satellite harmonics and integral formulas in physical geodesy, Gerlands Beitr. Geophysik, Leipzig 89(5):371-377.

Sjöberg L.E. (1981) Least-squares combination of terrestrial and satellite data in physical geodesy, Ann. Geophys., t. 37: 25-30.

Sjöberg L.E. (1984a) Least-Squares modification of Stokes' and Vening-Meinez' formula by accounting for truncation and potential coefficients errors. Manus. Geod., 9:209-229.

Sjöberg L.E. (1984b) Least-squares modification of Stokes' and Vening Meinesz' formulas by accounting for errors of truncation, potential coefficients and gravity data, Report No. 27, Department of Geodesy, Uppsala.

Sjöberg L.E. (1991) Refined least-squares modification of Stokes' formula, Manus. Geod. 16:367-375.

Sjöberg L.E. (2003) A general model for modifying Stokes' formula and its least-squares solution, J Geod. 77: 459–464.

Sjöberg L.E. and Eshagh M. (2009) Considering data gaps in geoid modeling by modifying Stokes's formula, *Submitted to Acta. Geod. Geophys. Hung*.

Tscherning C.C. and Rapp R. 1974. Closed covariance expressions for gravity anomalies, geoid undulations and deflections of vertical implied by anomaly degree variance models. Rep. 355. Dept. Geod. Sci. Ohio State University, Columbus, USA.

Tscherning C. C., Veicherts M. and Arabelos D. (2006) Calibration of GOCE gravity gradient data using smooth ground gravity, In Proc. GOCINA workshop, Cahiers de center European de Geodynamique et de seismilogie, Vol. 25, pp. 63-67, Luxenburg.

Wenzel, H.G. (1981) Zur Geoidbestimmung durch kombination von schwereanomalien und einem kugelfuncationsmodell mit hilfe von integralformeln. ZfV. 106, 3, p.102-111.

Wolf K. I. (2007) Kombination globaler potentialmodelle mit terresrischen schweredaten fur die berechnung der zweiten ableitungen des

gravitationspotentials in satellitenbahnhohe, PhD thesis, University of Hannover, Germany.

Zielinsky J.B. and Petrovskaya M.S. (2003) The possibility of the calibration/validation of the GOCE data with the balloon-borne gradiometer, Adv. in Geosci., 1:149-153.

Ågren J. (2004) Regional geoid determination methods for the era of satellite gravimetry, Numerical investigations using synthetic Earth gravity models, Doctoral thesis in Geodesy, Royal Institute of Technology, Stockholm, Sweden.